2021 43rd Annual International Conference of the
IEEE Engineering in Medicine & Biology Society (EMBC)
Oct 31 - Nov 4, 2021. Virtual Conference

Practical settings for shear wave speed estimation using the framework of Reverberant Shear Wave Elastography: A numerical simulation study

Gilmer Flores, Pierol Quispe, Stefano E. Romero, Juvenal Ormachea, and Benjamin Castaneda

Abstract— Reverberant shear wave elastography (RSWE) has become a promising approach to quantifying soft tissues' viscoelastic properties by the propagating shear wave speed (SWS) estimation based on the particle velocity autocorrelation. In this work, three different practical settings were evaluated for the SWS estimation by numerical simulations of an isotropic, homogenous, and elastic medium: first, the 2D representation of the particle velocity, second, the spatial autocorrelation computation, and third, the selection of the curve fitting domain. We conclude that the 2D autocorrelation function using the Wiener-Khinchin theorem provides up to 127 times faster results than traditional autocorrelation methods. Additionally, we state that extracting the magnitude and phase from the Fourier transform of the temporal domain, applying the 2D-autocorrelation on a mobile square window sized at least two wavelengths, and fitting the monotonically decreasing part of the autocorrelation profile's central lobe results in more accurate (13.2% of bias) and precise (5.3% of CV) estimations than other practical settings.

Clinical relevance— Affections in soft tissues' biomechanical properties are related to pathologies, such as tumor cancer, muscular degenerative diseases, or fibrosis. These changes are quantified by the SWS and its derived viscoelastic parameters. RSWE is a promising approach for their characterization. In this work, we evaluated alternative elections of practical settings within the methodology. Numerical simulations indicate they lead to faster and more reliable local SWS estimations than conventional settings.

I. Introduction

Reverberant shear wave elastography (RSWE) is a novel approach to assess quantitatively viscoelastic soft tissue parameters. It applies a narrow-band diffuse field of shear waves using multiple controlled external vibration sources. Their effects are augmented by naturally established reflections from anatomical boundaries and heterogeneities [1]. Hence, the particle velocity is modeled as a superposition of plane shear waves with random amplitude and phase, propagating in all directions. Consequently, local estimation of the wavenumber (k), and subsequently, the shear wave speed (SWS), could be obtained by calculating the spatial autocorrelation of the acquired particle velocity. Specifically, the axial and lateral profiles of the result are fitted to their respective theoretical functions, (2) and (3) reported on [2]. Fig. 1 shows the methodology used for the SWS estimation using this framework.

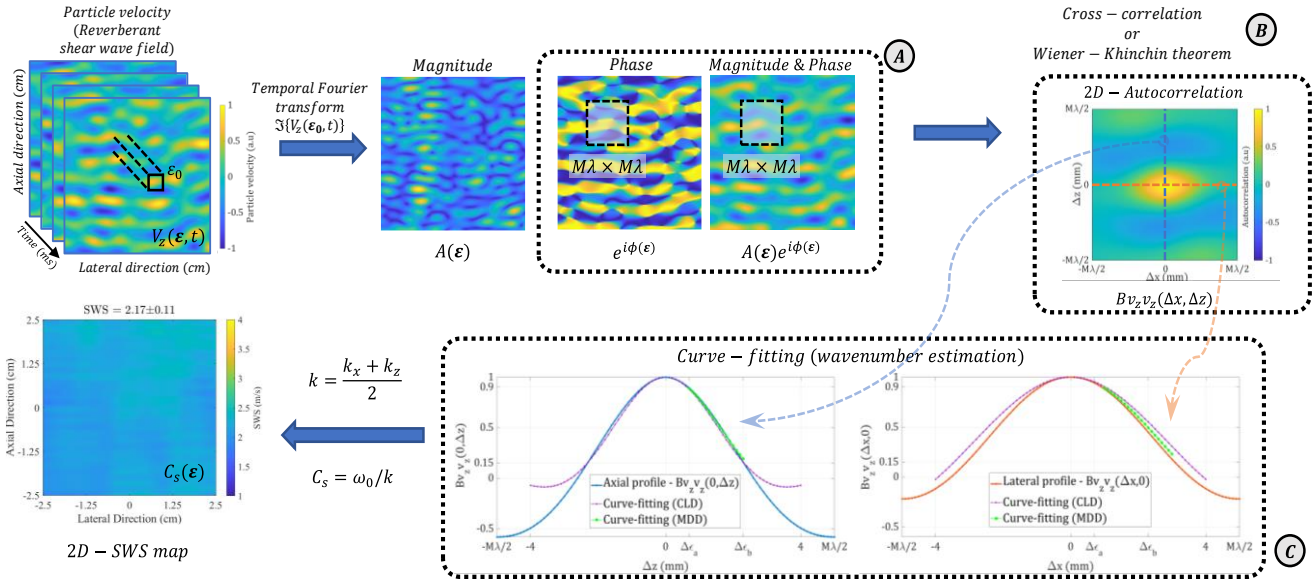

Figure 1. Methodology for the shear wave speed estimation. The 3D particle velocity (2D spatial, 1D temporal) can be represented by the 2D complex matrix (A - only phase or magnitude and phase) extracted from the temporal Fourier transform. Then, the spatial autocorrelation is calculated (B – by the Cross-correlation algorithm or using the Wiener-Khinchin theorem). Axial and lateral profiles are fitted to their respective theoretical functions (C – taking the curve's central lobe (CLD, purple dashed line) or the monotonically decreasing domain (MDD, green dashed line)) resulting in the wavenumber local estimation.

G. Flores, S. E. Romero, and B. Castaneda are with Laboratorio de imágenes médicas, Pontificia Universidad Católica del Perú, San Miguel, Lima, Perú (e-mail: sromerog@pucp.pe, gilmer.flores@pucp.edu.pe castaneda.b@pucp.edu.pe).

P. Quispe is with Biomedical Engineering Program PUCP-UPCH, Pontificia Universidad Católica del Perú, San Miguel, Lima, Perú, and Biomedical Engineering Program PUCP-UPCH, Universidad Peruana Cayetano Heredia, San Martín de Porres, Lima, Perú, (e-mail: pierol.quispe@pucp.edu.pe).

J. Ormachea is with Department of Electrical and Computer Engineering, University of Rochester, Rochester, NY, USA, (e-mail: jormache@ur.rochester.edu).

RSWE has shown promising results in the viscoelastic characterization of different tissues and has been implemented in ultrasound (US) and optical coherence tomography (OCT) [3]. However, following the methodology, different alternatives appear, such as the magnitude and phase extraction (A), window size, autocorrelation algorithms (B), and the curve-fitting's spatial domain selection (C), which imply different practical settings for shear wave speed estimation.

A. Magnitude and phase extraction

Magnitude and phase are extracted from the Fourier transform on the temporal domain as a complex representation of the continuous harmonic field in steady-state. Both have been used to apply the 2D-autocorrelation algorithm. Ormachea et al. [4] suggested the phase extraction setting the magnitude to the unit (Ph or $e^{i\phi(\varepsilon)}$), considering this as an idealization of an isotropic diffuse field. On the other hand, Zvietcovich et al. [2] used the magnitude and phase (Mg&Ph or $A(\varepsilon)e^{i\phi(\varepsilon)}$) as a reconstruction of the 2D spatial particle velocity in the axial component. In this work, these data selections were analyzed and compared.

B. Autocorrelation algorithm

A mobile squared window is used for calculating the corresponding 2D-autocorrelation. The window size effect on the estimation's accuracy and precision were evaluated by Zvietcovich et al. [5]. Their results indicated that the window should capture at least half wavelength and oversized windows produce reliable and repeatable speed estimation at the cost of losing lateral resolution. However, experiments with different vibration frequencies were not conducted. Moreover, they applied the autocorrelation by definition (cross-correlation algorithm or XC), which has $O(n^4)$ time complexity in Big-O notation, resulting in a high execution time and computational cost.

Conversely, the Wiener-Khinchin theorem (WKT) states that the Fourier transform (FFT) of a signal's autocorrelation is equal to the signal's power spectrum (the squared magnitude of the signal's Fourier Transform) [6]. Thus, the 2D-autocorrelation could be obtained by applying the inverse Fourier transform (2D-IFFT) to the element-wise product of the window's 2D- FFT with the respective conjugate. Thus, its time complexity is reduced to $O(n^2 log_2 n)$.

Hence, we propose the WKT as an autocorrelation algorithm to obtain the same result as XC but with a lower execution time.

C. Curve-fitting spatial domain.

In previous works, the curve-fitting is limited to the domain in which the autocorrelation profiles' central lobe (CLD) is selected. The coefficient of determination (R^2) is chosen as a goodness of fit [7]–[9]. However, this parameter does not work correctly with nonlinear models [10], making the analysis incomplete and biased. We proposed to limit the domain for positive values and use the monotonically decreasing part of the central lobe (MDD) since it could be approximated to a linear function. In that sense, problematic patterns in residual values are eliminated within this restricted domain of the model, and the obtained R^2 becomes a reliable parameter to assess the fitting.

This work compares the different alternatives we explained lines above to estimate the SWS in elastic isotropic homogeneous media. We conducted numerical simulations in which plane shear waves with three different wavenumbers polarize the specified medium.

II. Methods

Numerical simulations were performed in MATLAB (version R2019b, MathWorks Inc., Natick, MA, USA) using a Monte Carlo method. The mathematical model used is based on a summation of 60 incident shear waves (minimum value to obtain a reverberant field [7]) where the uniformly distributed random input variables considered were the propagation direction vector, the displacement direction vector, which depend on the parameters in spherical coordinates, the magnitude of the particle displacement speed ([0,1] m/s) and the phase ([0, 2π] rad). The applied vibration frequencies (f_v) were 300, 400, and 500 Hz since these are commonly used in RSWE experiments [11]. This medium's elasticity was established by the shear wave speed (SWS or C_s) equal to 2.5 m/s. The reverberant field is formed within a cubic medium with a resolution ($\Delta\varepsilon$) equal to 0.1 mm.

First, each alternative (A, B, and C) was evaluated with a single estimation using a window placed at the medium's central point. The squared window size was selected as a wavelength function. Explicitly, the side was "M" times the correspondent λ where $M\lambda = \{0.5\lambda; 0.75\lambda; 1\lambda; 1.5\lambda; 2\lambda; 3\lambda; 4\lambda; 5\lambda\}$. One hundred events per scenario were carried out iteratively.

A. Magnitude and phase extraction

The accuracy and precision of two data selection alternatives were evaluated: first, the extracted magnitude and phase and, second, the phase with the magnitude set to the unit. Curve fittings are applied to the extracted, corrected, and normalized 2D-autocorrelation profiles using the cross-correlation algorithm. Only the points belonging to the central region of these functions were considered. Thus, for each direction, the wavenumbers (k), the underlying value of the SWS, the coefficients of determination (R^2), the relative errors, and the standard deviations were estimated.

B. Autocorrelation algorithm

The cross-correlation (XC) and the Wiener-Khinchin theorem (WKT) algorithms for the 2D autocorrelation were compared. The computation time's mean, standard deviation, and median were calculated and compared with the expected computation times T_{XC} and T_{WKT}, which are [6]

$$T_{XC}(n) = a_0 n^4, \text{ and} \quad (1)$$

$$T_{WKT}(n) = b_0 n^2 \log_2 n, \quad (2)$$

where $n = M\lambda/\Delta\varepsilon$, represents the square matrix's size, and a_0 and b_0 are time constants, obtained by fitting the execution time's means with (1) and (2).

C. *Curve-fitting spatial domain*

The curve-fitting to the theoretical functions were applied using the domain established by $[\Delta\varepsilon_a; \Delta\varepsilon_b] > 0$, where $Bv_zv_z(\Delta\varepsilon_a) \cong 0.9$ and $Bv_zv_z(\Delta\varepsilon_b) \cong 0.15$, representing the monotonically decreasing part of the central lobe. The precision and accuracy of the SWS and R^2 were evaluated.

Finally, the proposed alternatives were unified for 2D-SWS map estimation and compared with a conventional election of alternatives.

III. Results

Fig. 2 shows the SWS estimation and R^2 (lateral and axial results were averaged) using the different methodologies mentioned in Section II.A applying different vibration frequencies (300, 400, and 500 Hz). In general, the magnitude and phase extraction ($A(\varepsilon)e^{i\phi(\varepsilon)}$) resulted in a more accurate and precise estimation.

Fig 3. shows the results of the computed autocorrelation function using XC and WKT. Axial and lateral profiles were extracted from aleatory events. Both operators provide similar results (only 400 Hz experiments were presented for space limitation). However, WKT's computation time is significantly lower than XC's (up to 127erg times faster), as shown in Fig. 4. Additionally, the expected computation time from (1) and (2) was calculated, finding $a_0 = 2.79\times10^{-10}$ and $b_0 = 5.68\times10^{-8}$.

The comparison between selecting the whole central lobe domain (CLD) and choosing the monotonically decreasing part of the central lobe (MDD) is presented in Fig 5. The SWS estimation and R^2 were compared, showing that estimations are repeatable using the MDD. However, they are down-biased for window sizes smaller than 2λ.

Two 2D-SWS maps were created to compare the proposed alternatives with the previously used methodology. Table II enumerates the difference between both images, which are presented in Fig. 6.

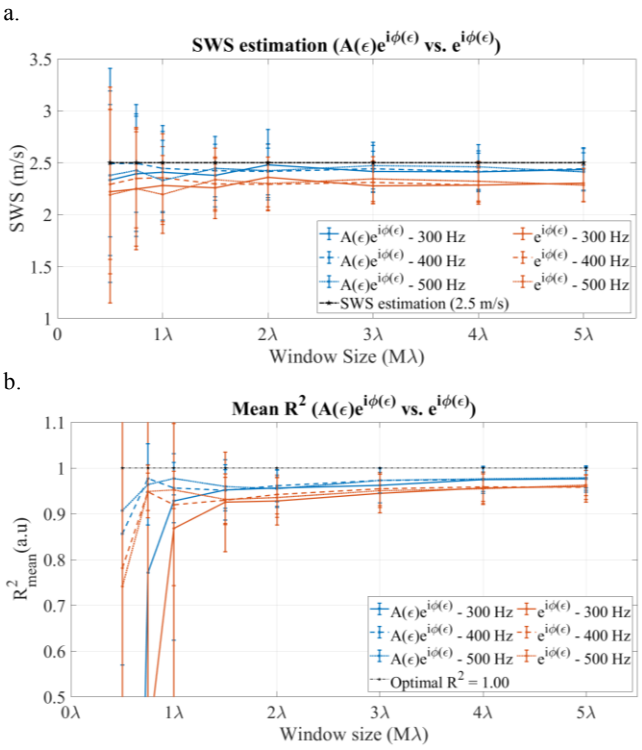

Figure 2. (a.) SWS and (b.) Mean R^2 using both alternatives of data processing: Magnitude and phase $A(\varepsilon).e^{i\phi(\varepsilon)}$ or only phase extraction $e^{i\phi(\varepsilon)}$

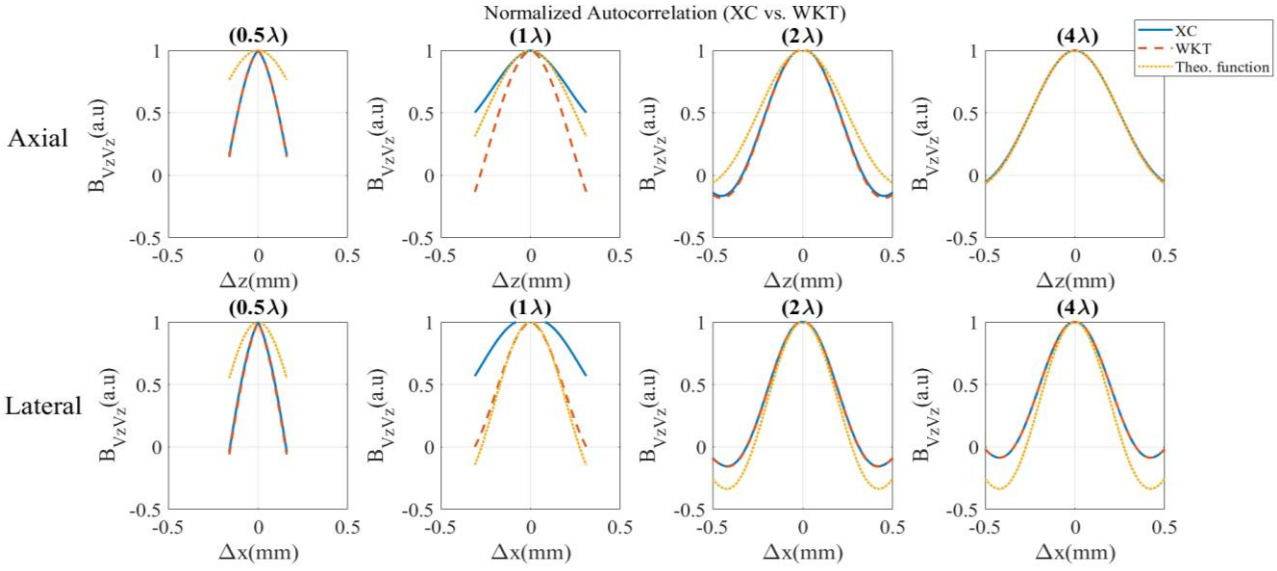

Figure 3. Computed autocorrelation function using the cross-correlation definition (XC) and the Wiener-Khinchin theorem (WKT) applied in different window sizes (0.5λ, 1λ, 2λ and 4λ, where λ=SWS/f_v and f_v = 400Hz). Axial (top) and lateral (bottom) extracted profiles are compared with their respective theoretical function.

a.

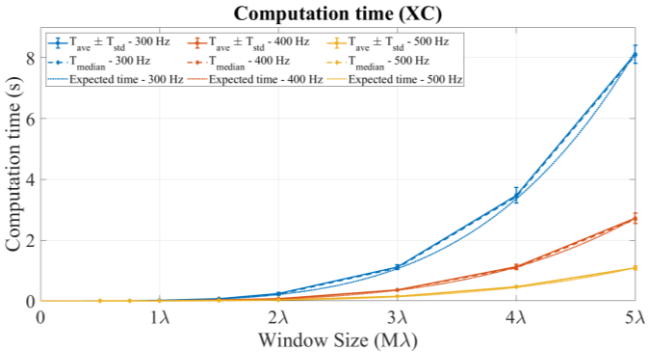

b.

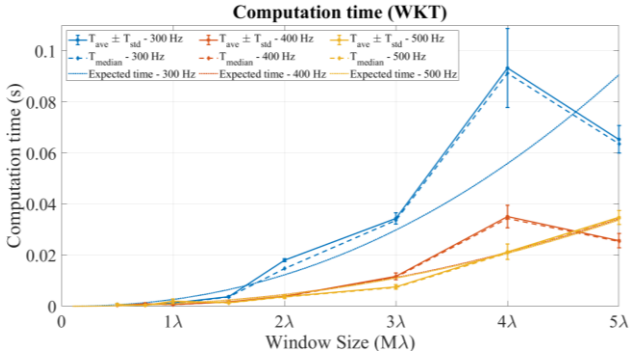

Figure 4. Computation time as a result of using XC (a.) and WKT (b.) as window size functions.

IV. Discussion

First, both data selection alternatives for image processing to obtain the RSWE estimator were compared. The magnitude and phase extraction resulted in a more accurate and precise alternative than selecting only the phase and setting the magnitude to unity. The results are supported with the R^2 values nearer to 1 for Mg&Ph. It could be explained by observing the images representing the particle velocity and their respective spatial spectrum (Fig. 7). Ph presents abrupt local changes drawing on high spatial frequency (wavenumber) components and, thus, a down-biased SWS estimation. The opposite occurs with Mg&Ph, which presents smooth changes in the particle velocity and lower wavenumber components.

Second, applying the Wiener-Khinchin theorem to calculate the 2D-autocorrelation function gives the same results as utilizing the cross-correlation definition but faster computation time (up to 127 times faster for the largest window size experiment). It was predicted by (1) and (2), which derive from their respective Big-O notation [6], [12]. In that sense, the advantage of reducing the computation time leads to a rapid implementation for real-time clinical applications.

Third, previous literature [6], [9] refers that the R^2 is an essential but not sufficient parameter to assess the SWS estimation quality. However, the nonlinear models of the autocorrelation profiles lead to unpredictable situations. Hence, the MDD is presented as a solution that presents precise SWS estimation and a coherent R^2 since MDD could be approximated to a linear model. Nevertheless, an analytic selection of a linear domain will be a future investigation endeavor.

Fourth, different window sizes were evaluated. As [5] indicated, larger windows present accurate and precise estimation, which leads to repeatable and reliable results. It could be explained since a shorter window size means fewer spatial samples to calculate the autocorrelation.

Finally, a comparison between the 2D-SWS map construction was performed to demonstrate the significant differences between choosing the proposed alternatives (map 1) and selecting others (map 2). A homogeneous result appears on map 2, representing a better estimation for the simulated medium's characteristics. It is also supported by a mean R^2 near to the unity and with a low standard deviation. Additionally, even with a larger window size, map 2 presented a lower computation time (1.16 times faster).

a.

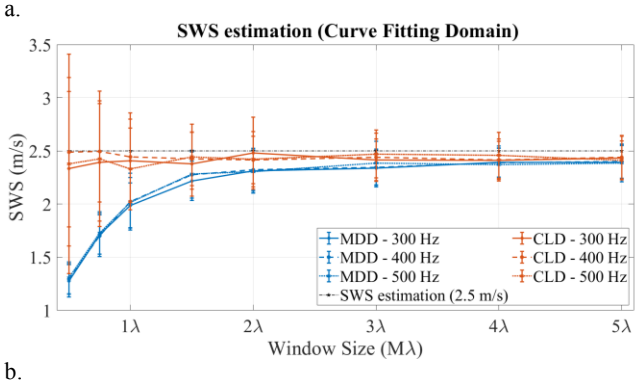

b.

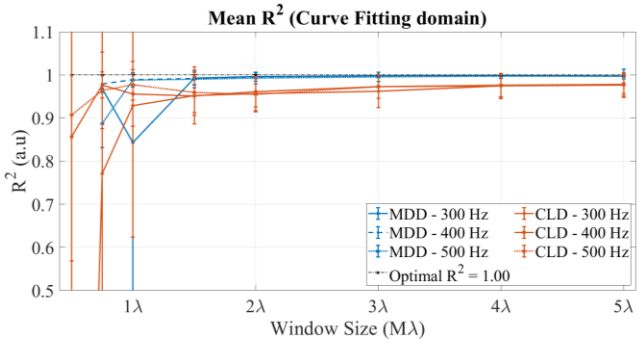

Figure 5. SWS estimation (a.) and mean R^2 (b.) with CLD and MDD.

TABLE I. Differences of Image Processing for SWS Maps Formation

	Map 1	**Map 2**
Selected Data	$e^{i\phi(\varepsilon)}$	$A(\varepsilon)e^{i\phi(\varepsilon)}$
Autocorrelation algorithm	XC	WKT
Curve-fitting spatial domain	CLD	MDD
Window size	1λ	3λ
Vibration frequency	400 Hz	
Mean SWS +/- STD*	1.67 ± 0.30 m/s	2.17 ± 0.11 m/s
Bias / CV**	33.4% / 18.2%	13.2% / 5.3%
Mean R^2 +/- STD*	0.76 ± 0.20	0.97 ± 0.09
Computation time	7271.7 s	6287.5 s

*STD: Standard deviation, **CV: Coefficient of variation

V. Conclusion

Three different practical settings for the SWS estimation using the RSWE framework were analyzed and compared by numerical simulations of a specific medium: isotropic, uniform, and elastic medium. A faster (up to 127 times) and reliable (5.3% of CV) estimation can be achieved by applying the proposed setting: using the monotonically decreasing part of the autocorrelation functions obtained by applying the Wiener-Khinchin theorem to a moving square window, with a size at least two times the predicted wavelength, throughout the image representing the extracted magnitude and phase.

Acknowledgment

G.Flores and P.Quispe thank Laboratorio de Imagenes medicas' members for their friendship, advice, and support. The PUCP Research Period Award supported B. Castaneda.

References

[1] K. J. Parker, J. Ormachea, F. Zvietcovich, and B. Castaneda, "Reverberant shear wave fields and estimation of tissue properties," *Physics in Medicine and Biology*, vol. 62, no. 3, pp. 1046–1061, 2017.

[2] F. Zvietcovich, P. Pongchalee, P. Meemon, J. P. Rolland, and K. J. Parker, "Reverberant 3D optical coherence elastography maps the elasticity of individual corneal layers," *Nature Communications*, vol. 10, no. 4895, pp. 1–13, 2019.

[3] J. Ormachea and F. Zvietcovich, "Reverberant Shear Wave Elastography: A Multi-Modal and Multi-Scale Approach to Measure the Viscoelasticity Properties of Soft Tissues," *Frontiers in Physics*, vol. 8, Jan. 2021.

[4] J. Ormachea, B. Castaneda, and K. J. Parker, "Shear wave speed estimation using reverberant shear wave fields: Implementation and feasibility studies," *Ultrasound in Medicine and Biology*, vol. 44, no. 5, pp. 963–977, 2018.

[5] F. Zvietcovich, P. Pongchalee, P. Meemon, J. P. Rolland, and J. Parker, "Supplementary information for : ' Reverberant 3D Optical Coherence Elastography (Rev3D-OCE): A novel method for the elasticity mapping of individual layers in cornea .'"

[6] K. M. Aamir and M. A. Maud, "Recursive Wiener-Khintchine Theorem," vol. 1, no. 2, pp. 418–420, 2007.

[7] G. Flores, J. Ormachea, S. E. Romero, F. Zvietcovich, K. J. Parker, and B. Castaneda, "Experimental study to evaluate the generation of reverberant shear wave fields (R-SWF) in homogenous media," in *2020 IEEE International Ultrasonics Symposium (IUS)*, 2020, pp. 1–4.

[8] A. Tecse, S. Romero, G. Flores, and B. Castaneda, "Bidimensional analysis of reverberant shear wave elastography with multiple aleatory mini-surface sources: simulation study," in *16th International Symposium on Medical Information Processing and Analysis*, 2020, vol. 11583, p. 115830V.

[9] R. Naemi *et al.*, "Diabetes Status is Associated With Plantar Soft Tissue Stiffness Measured Using Ultrasound Reverberant Shear Wave Elastography Approach," *Journal of Diabetes Science and Technology*, p. 1932296820965259, Oct. 2020.

[10] A. N. Spiess and N. Neumeyer, "An evaluation of R2as an inadequate measure for nonlinear models in pharmacological and biochemical research: A Monte Carlo approach," *BMC Pharmacology*, 2010.

[11] E. Machado, S. E. Romero, G. Flores, and B. Castaneda, "Feasibility of Reverberant Shear Wave Elastography for In Vivo Assessment of Skeletal Muscle Viscoelasticity," in *2020 IEEE International Ultrasonics Symposium (IUS)*, 2020, pp. 1–4.

[12] C.-C. Shen, Y.-Q. Xing, and G. Jeng, "Autocorrelation-based generalized coherence factor for low-complexity adaptive beamforming," *Ultrasonics*, vol. 72, pp. 177–183, 2016.

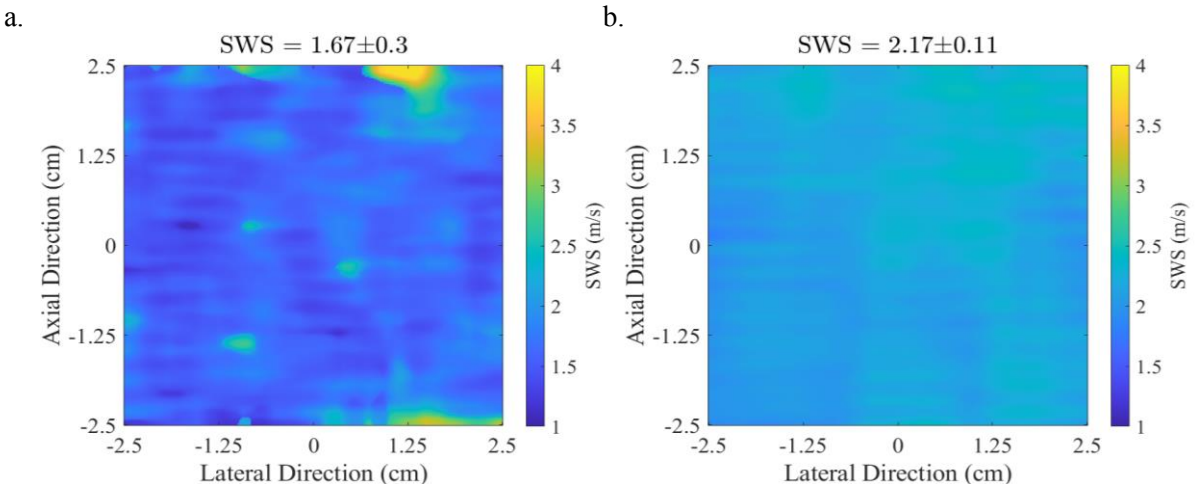

Figure 6. 2D-SWS map construction. Comparison between Map 1 (a.) and Map 2 (b.)

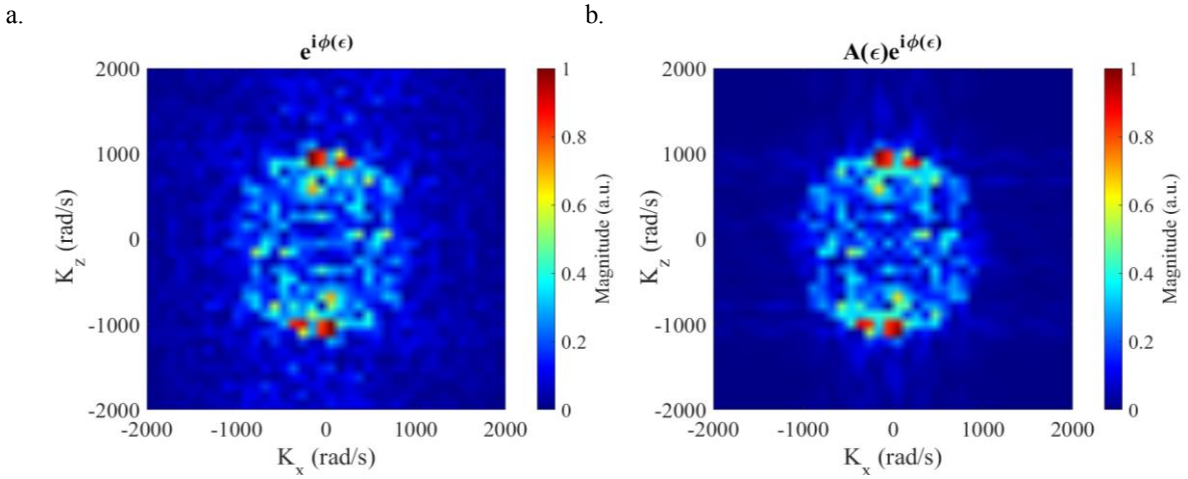

Figure 7. Spatial frequency spectra of Ph (a.) and Mg&Ph (b.) show a centered circle with radius approximately equal to the selected wavenumber.